Supporting Information

Supramolecular recognition enhanced electrochemical sensing: β-cyclodextrin and Pd nanoparticles co-decorated 3D reduced graphene oxide nanocomposites modified glassy carbon electrode for quantification of ractopamine

Kai Zhang [a], Xiaoyuan Zhang [a], Yanqin Rong [*a], Qingfang Niu [a], Pengyue Jin [b], Xuewen Ma [*a], Cheng Yang [b], Wenting Liang [*a]

a. Institute of Environmental Science, School of Chemistry and Chemical Engineering, Shanxi University, Taiyuan, 030006, China. Email: ryanqin0328@163.com (Y. R.); maxuewen@sxu.edu.cn (X. M.); liangwt@sxu.edu.cn (W. L.).

b. Key Laboratory of Green Chemistry & Technology of Ministry of Education, Sichuan University, Chengdu 610064.

Fabrication process of the 3D-rGO/Pd/β-CD hybrids

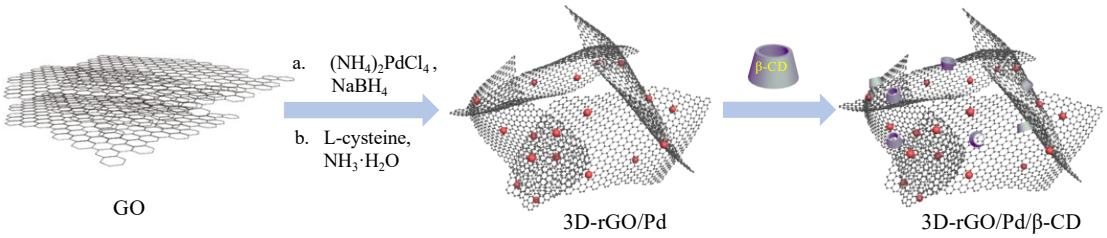

Scheme S1 The synthesis route of 3D-rGO/Pd/β-CD

Characterization of the 3D-rGO/Pd/β-CD

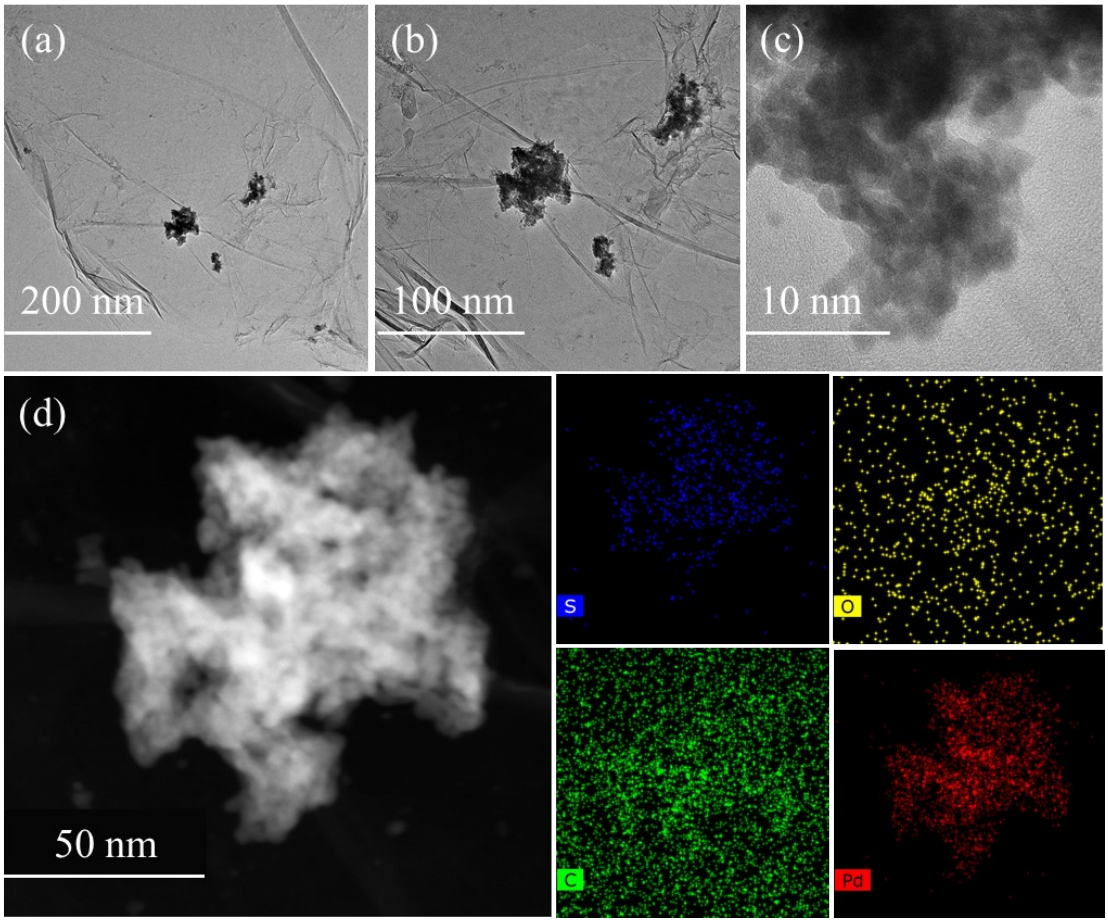

Fig. S1 TEM images at the same magnifications and EDS elemental mapping of C, O, S and Pd of 3D-rGO/Pd.

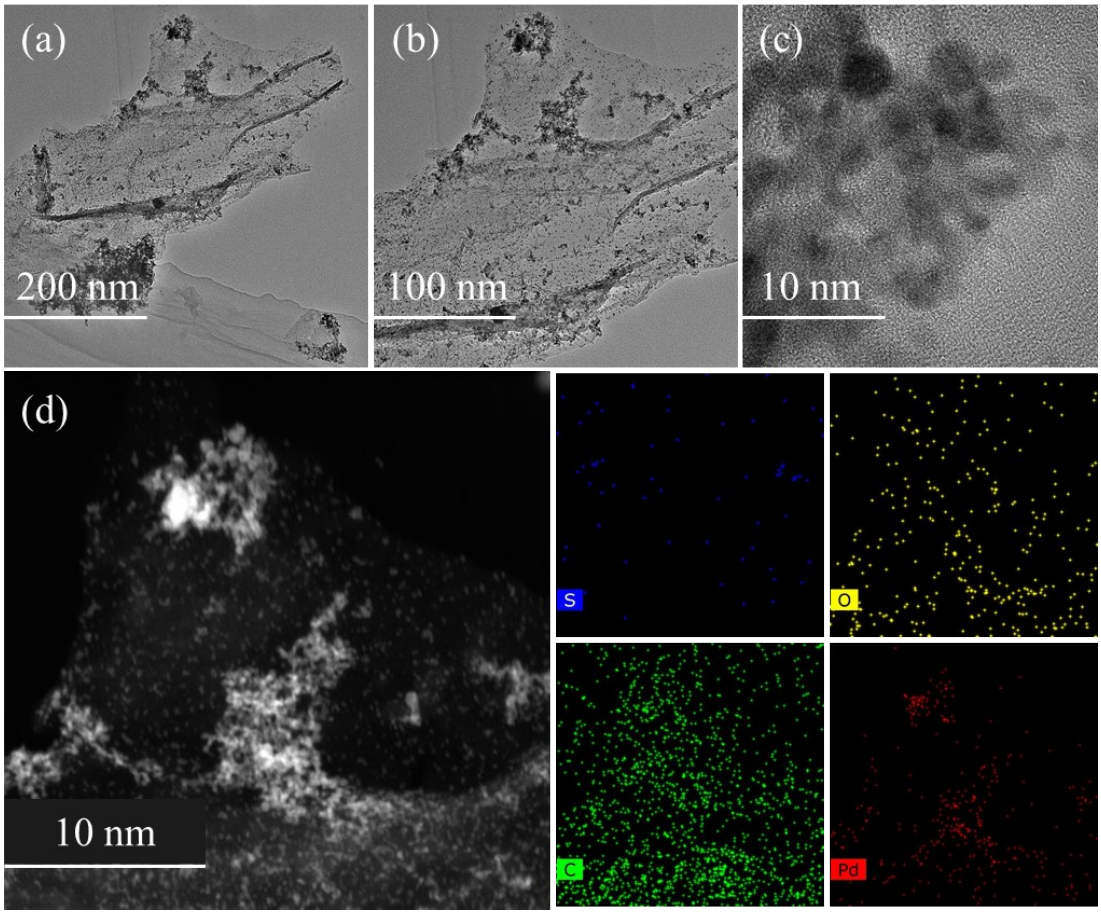

Fig. S2 TEM images at the same magnifications and EDS elemental mapping of C, O, S and Pd of 3D-rGO/Pd/β-CD.

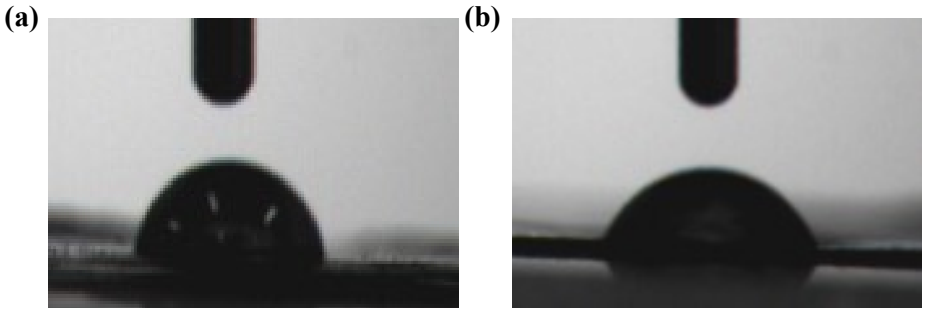

Fig. S3 Contact-angle photographs of 3D-rGO/Pd (a) and 3D-rGO/Pd/β-CD (b) modified substrates.

Optimization of recognition conditions

Influence of sweep speed

In order to explore the reaction mechanism of RAC on the electrode surface, the relationship between scanning rate (v) and peak current (I) was investigated by CV. As shown in Fig. S4a, it can be seen that there are only oxidation peaks in the CV curve, indicating that RAC at 3D-rGO/Pd/β-CD/GCE is irreversible [1]. At the same time, the electrochemical response signal of 3D-rGO/Pd/β-CD/GCE towards RAC increases linearly with the scanning rate (Fig. S4b), corresponding to the linear equation I (μA) = 188.4475 v + 1.8426 (R^2 = 0.9922), confirming that the oxidation process of RAC is subject to surface adsorption control. In addition, the peak potential (E_{pa}) of the RAC moves slowly toward the positive potential, which is also logarithm to the sweep rate to present a linear positive correlation (Fig. S4c), the corresponding equation is E_{pa} = 0.0759 log v + 0.6694 (R^2 = 0.9902). According to Laviron's theory [2]:

$$E_{pa} = E^{0'} + \left(\frac{2.303RT}{\alpha n_a F}\right)\log\left(\frac{RTK^0}{an_aF}\right) + \left(\frac{2.303RT}{an_aF}\right)\log v \quad (1)$$

where $E^{0'}$ is the standard voltage, T is the temperature, α is the electron transfer constant, n_a is the number of electrons transferred, K^0 is the standard Heterogeneous electron transfer rate constant, F is Faraday's constant, and the value of α usually is assumed to be 0.5 in an irreversible electrochemical reaction. Combining the linear equation and the Laviron equation, αn_a = 0.8162 can be calculated, so it is known that there are two electrons involved in the oxidation process of the RAC.

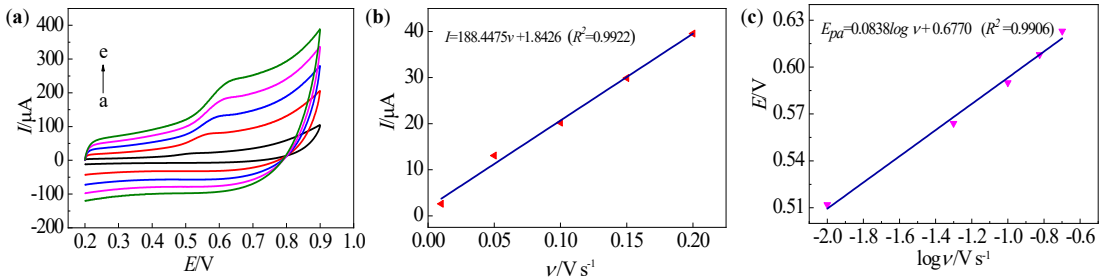

Fig. S4 (a) Influence of different scan rates (a-e: 0.01, 0.05, 0.1, 0.15, 0.2 V s^{-1}) on the peak current for the determination towards 50 μM RAC of 3D-rGO/Pd/β-CD/GCE; (b) The linear relationship between scan rate and peak current of RAC; (c) The linear relationship between the peak potential of RAC and the logarithm of scan rate (log v/V s^{-1})

Influence of the pH

The pH value in the electrolyte solution plays an important role in the electrochemical detection process. The influence of different pH values ranging from 4.0 to 9.0 on the electrical response signals of RAC was studied by DPV. As shown in Fig. S5a, b, it is found that the peak current of RAC first increase and then decrease in the pH range from 4.0 to 9.0, and the maximum of peak current occurs at pH 8.0. However, the solubility of RAC in PBS solution at pH = 8 decrease compared with that at pH = 7, and in order to be close to the physiological liquid environment, pH = 7 is an optimal value for subsequent experiments. In addition, the relationship between pH and E_{pa} value is explored, as shown in Fig. S5c, the pH value increases gradually, and the oxidation peak potential turns negative gradually, which indicates that proton transfer occurs during the reaction of RAC. The pH and E_{pa} values also have a better linear relationship, and the corresponding fitting equation is E = 1.0312 - 0.0747 pH (R^2 = 0.9833). The following is the pH dependence equation of the oxidation peak potential (E_{pa}) of RAC [3]:

$$E_{pa} = E^0 - (2.303mRT/nF)\text{pH} \quad (2)$$

Where E^0 is the standard redox potential, m and n are the number of protons and electrons involved in the redox process, respectively. The other parameters all indicate the normal meaning. The slope of the linear equation measured in practice is 0.0765, which is close to the theoretical slope of 0.0592. It can be concluded that the transferred electron number in RAC electrochemical oxidation process equals to the amount of proton transfer. Therefore, combined with the result of the upper experiment, we further infer that the electrochemical oxidation reaction of RAC was accompanied by the transfer of two protons and electrons due to the occurrence of the oxidation process from the phenolic hydroxyl group at the end of the RAC molecule. The electrochemical oxidation mechanism corresponding to RAC with 3D-rGO/Pd/β-CD/GCE is shown in Scheme S1, which was consistent with other reported literature.[1,4]

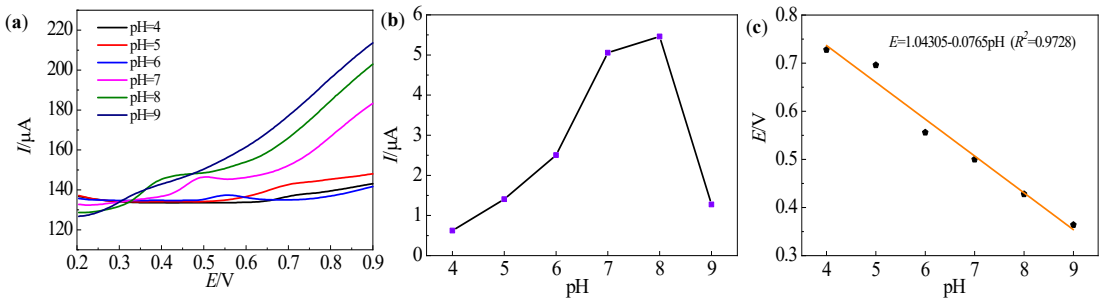

Fig. S5 (a) Influence of pH on the peak current for the determination towards 50 μM RAC of 3D-rGO/Pd/β-CD/GCE; (b) The relationship between pH and the oxidation peak current; (c) The relationship between pH and the peak potential

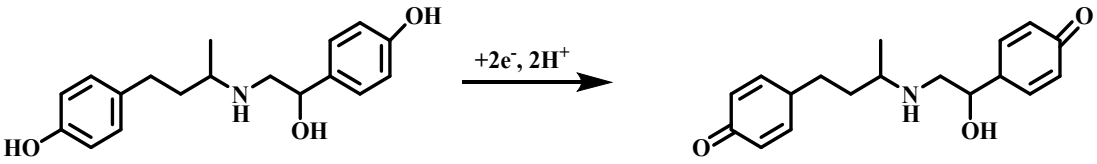

Scheme S2 The electrochemical oxidation mechanism for the determination towards RAC of 3D-rGO/Pd/β-CD/GCE

Influence of the modification amount of 3D-rGO/Pd/β-CD

The film thickness of the modified materials has a close relationship with electron transfer and mass diffusion. Therefore, controlling the thickness of the sensing film is crucial, and the modification amount of 3D-rGO/Pd/β-CD dispersion on the peak current signal of RAC was further examined (Fig. S6a). As shown in Fig. S6a, it is evident that the current response has a maximum value when the modification amount is 5 μL. Therefore, 5 μL of 3D-rGO/Pd/β-CD was applied to be immobilized on the GCE surface.

Influence of the accumulation time

The influence of accumulation time on RAC detection by 3D-rGO/Pd/β-CD/GCE was also investigated. As shown in Fig. S6b, with regard to RAC, the peak current increases gradually with extending the incubation time from 0 to a maximum at 120 s, and decreases successively with the raise of the time up to 150 s, implying the achievement of adsorption equilibrium of RAC on the surface of the electrode. Therefore, 120 s is used as the optimal accumulation time.

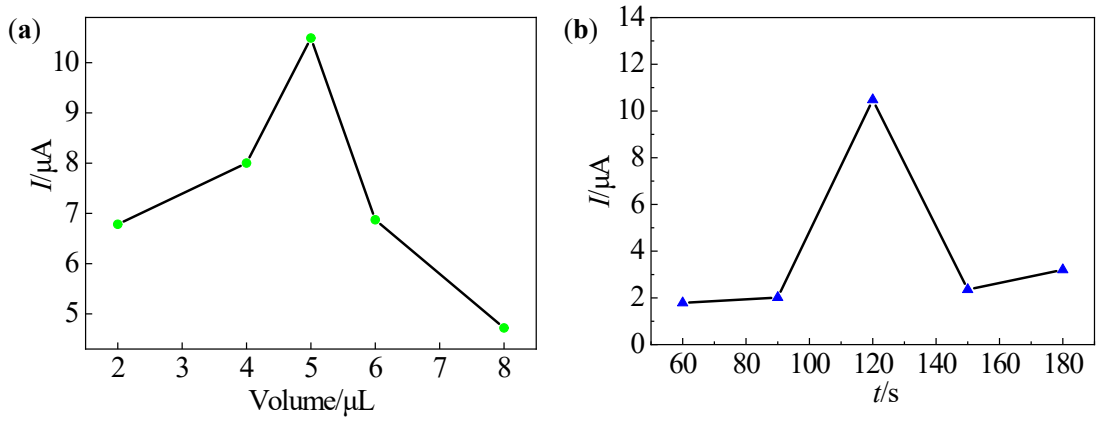

Fig. S6 Influence of volume (a) and time (b) on the peak current for the determination towards 50 μM RAC of 3D-rGO/Pd/β-CD/GCE

Approach for determining the limit of detection (LOD)[5-7]

LOD is calculated using the formula of LOD = 3*S*/*b* according to a linear calibration equation and the signal-to-noise ratio *S*/*N*=3 following IUPAC definition. Therein, *S* is the standard deviation of the blank experiment and *b* is the slope of the calibration plot towards RAC. In detail, the value for *S* was given through running parallel determination for ten times in blank electrolytes at 3D-rGO/Pd/β-CD/GCE, and *b* was slope value 0.3933 μA μM^{-1} for the first liner segment towards RAC. Putting the corresponding values in the above equation obtains the LOD.

Job's plot determination

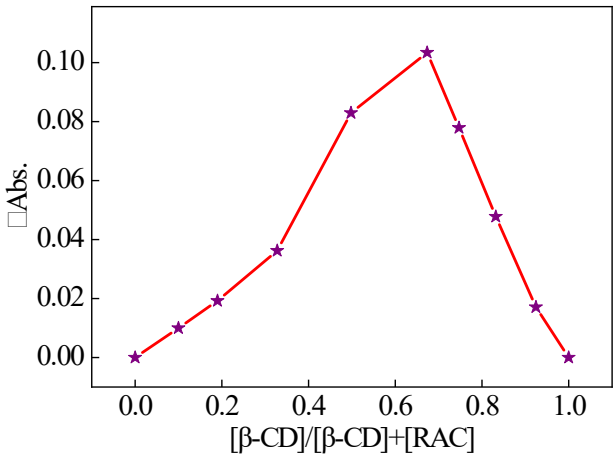

Fig. S7 The obtained Job's plot curve (λ = 273 nm)

Table S1 Comparison of different materials by using different methods for the determination of RAC

Materials	Techniques	Linear range (μM)	LOD (μM)	References
Fe_3O_4/rGO-MSPE	DPV	0.05-100	0.013	2
NBC/GCE	DPV	0.1-1.75	0.041	8
$PMEO_2MA/C_{60}$-rGO/GCE	DPV	0.1-3.1	0.082	9
Ag_2TPPS_4/AgNPs/ng-C_3N_4/GCE	DPV	0.1-12	0.051	10
S-β-CD-BP-PEDOTs/GCE	DPV	0.3-9.4	0.12	11
Nafion/HPMo/MoS_2/PDDA/GCE	DPV	1-70	0.056	12
NPVMo/ZrO_2/GCE	DPV	3-50	0.93	13
Apt/HKUST-1/PTC-PEI/GCE	ECL	1×10^{-6}-1.0	6.17×10^{-7}	14
$Mn_3(PO_4)_2$@BSA@AuNPs	EIS	2.9×10^{-5}- 0.296	7.7×10^{-5}	15
MCF/CPE	LSV	0.05-3	0.01	16
DPA-GQDs	Fluorescence	0.83-49.8	0.83	17
AuNPs@COFs/GCE	Amperometry	1.2-1600	0.12	18
PoAT-AuNP-Au electrode	QCMs[a]	2.5-150	1.17	19
SiW_9Cu_3	Colorimetry	156-373	79.4	20
3D-rGO/Pd/β-CD/GCE	DPV	1-95	0.12	This work

[a] Quartz crystal microbalances (QCMs)

Table S2 Comparison of repeatability and stability of RAC by electrochemical detection using different electrodes

Electrodes	Repeatability (times)	RSD	Stability (days)	Percentage of the initial response	References
COOH-GN/Jps/Apt/BSA/GCE	10	0.28%	14	> 95.0%	21
NBC/GCE	6	2.6%	25	95.25%	8
AuNPs@COFs/GCE	6	0.51%	15	96.4%	18
PoAT-AuNP-Au electrode	5	4.8%	30	82%	19
Bi_2Te_3@g-C_3N_4 BNs/GCE	10	—	30	—	1
Fe_3O_4/rGO-MSPE	—	—	28	89.63%	8
3D-rGO/Pd/β-CD/GCE	4	4.97%	20	94.25%	This work

Table S3 Determination of RAC in pork samples with 3D-rGO/Pd/β-CD/GCE

Real Sample	Original	Added (μM)	Found (μM)	Recovery (%)	RSD (%)
1	0.00	8.00	8.27	103.99	3.37
2	0.00	15.00	15.76	103.42	5.06
3	0.00	20.00	19.75	99.27	1.25
4	0.00	50.00	48.22	96.44	3.56

Table S4 ^{1}H NMR chemical shifts (δ) of β-CD in the absence and presence of RAC

β-CD protons	δ_{free} (ppm)	$\delta_{complex}$ (ppm)	Δδ (ppm)
H_a	5.003	4.998	-0.015
H_c	3.898	3.654	-0.244
$H_{e,\ f}$	3.807	3.793	-0.014
H_b	3.583	3.588	0.005
H_d	3.517	3.511	-0.006

Table S5 ^{1}H NMR chemical shifts (δ) of RAC in the absence and presence of β-CD

RAC protons	δ_{free} (ppm)	$\delta_{complex}$ (ppm)	Δδ (ppm)
H_2	7.205	7.246	0.041
H_{10}	7.104	7.077	-0.027
H_1	6.854	6.852	-0.002
H_{11}	6.793	6.748	-0.045
H_5	4.831	4.890	0.059
H_3	4.775	4.847	0.072
H_6	3.229	3.253	0.024
H_9	3.153	3.170	0.017
H_4	2.594	2.638	0.044
H_8	1.973, 1.792	2.055, 1.800	0.082, 0.008
H_7	1.301	1.281	-0.020

References

1 U. Rajaji, T. W. Chen, S. Chinnapaiyan, S. M. Chen and M. Govindasamy, *Anal. Chim. Acta*, 2020, **1125**, 220–230.

2 Y. Poo-arporn, S. Pakapongpan, N. Chanlek and R. P. Poo-arporn, *Sensor. Actuat. B*, 2019, **284**, 164–171.

3 X. Liu, W. J. Wang, X. Q. Li, C. J. Li, L. X. Qin, Ji Sun and S. Z. Kang, *Electrochim. Acta*, 2016, **210**, 720–728.

4 K. K. Li, J. R. Cui, Q. Yang, S. L. Wang, R. M. Luo, A. Rodas-Gonzalez, P. Y. Wei and L. Liu, *Food Chem.*, 2023, **405**, 134791.

5 Y. Wang, Y. Q. Chen, H. Bian, Y. W. Sun, L. J. Zhu and D. H. Xia, *Sensor. Actuat. B*, 2021, **341**, 130044.

6 P. Lei, Y. Zhou, R. Q. Zhu, Y. Liu, C. Dong and S. M. Shuang, *Biosens. Bioelectron.*, 2020, **147**, 111735.

7 M. Zheng, Y. Wang, C. Wang, W. Wei, S. Ma, X. Sun and J. He, *Spectrochim. Acta A*, 2018, **19**, 315–321.

8 L. P. Cao, Q. Ding, M. H. Liu, H. T. Lin and D. P. Yang, *ACS Appl. Bio. Mater*., 2021, **4**, 1424−1431.

9 C. Chen, M. X. Zhang, C. Y. Li, Y. X. Xie and J. J. Fei, *Microchim. Acta,* 2018, **185**, 155.

10 X. H. Weng, H. L. Ye, W. Q. Xie, M. H. Ying, H. B. Pan and M. Du, *Nanoscale Adv*., 2021, **3**, 3900.

11 Y. Ge, M. Qu, L. Xu, X. Wang, J. Xin, X. Liao, M. Li, M. Li and Y. Wen, *Microchim. Acta*, 2019, **186**, 836.

12 Q. W. Wang, M. Wang, N. Zhang, X. Huang, X. Wang and S. Wang, *Microchem. J.*, 2023, **189**, 108434.

13 L. H. Zhang, Q. W. Wang, Y. Qi, L. Li, S. T. Wang and X. H. Wang, *Sensor. Actuat. B*, 2019, **288**, 347–355.

14 L. J. Zhou, D. Jiang, Y. R. Wang, H. B. Li, X. L. Shan, W. C. Wang and Z. D. Chen, *Analyst*, 2021, **146**, 2029–2036.

15 Z. Zhang, Y. Zhang, R. Song, M. Wang, F. Yan, L. He, X. Feng, S. Fang, J. Zhao and H. Zhang, *Sensor. Actuat. B*, 2015, **211**, 310–317.

16 L. P. Xie, Y. Ya and L. Wei, *Int. J. Electrochem. Sci.*, 2017, **12**, 9714–9724.

17 K. Sadinejad, A. Mirzaie, P. Pashazadeh-Panahi and M. Hasanzadeh, *J. Mol. Recognit.*, 2021, **34**, e2903.

18 S. Y. Yang, R. X. Yang, J. Y. He, Y. Zhang, Y. H. Yuan, T. L. Yue and Q. L. Sheng, *Foods*, 2023, **12**, 842.

19 L. J. Kong, M. F. Pan, G. Z. Fang, X. L. He, Y. K. Yang, J. Dai and S. Wang, *Biosens. Bioelectron.*, 2014, **51**, 286–292.

20 X. X. Duan, Z. X. Bai, X. T. Shao, J. Xu, N. Yan, J. Y. Shi and X. H. Wang, *Materials*, 2018, **11**, 674.

21 Y. Zhou, T. T. Wang, L. T. Yan, G. M. Zhang, Y. Zhang, C. H. Zhang and S. M. Shuang and Y. J. He, *Chinese J. Anal. Chem*., 2022, **50**, 100056.